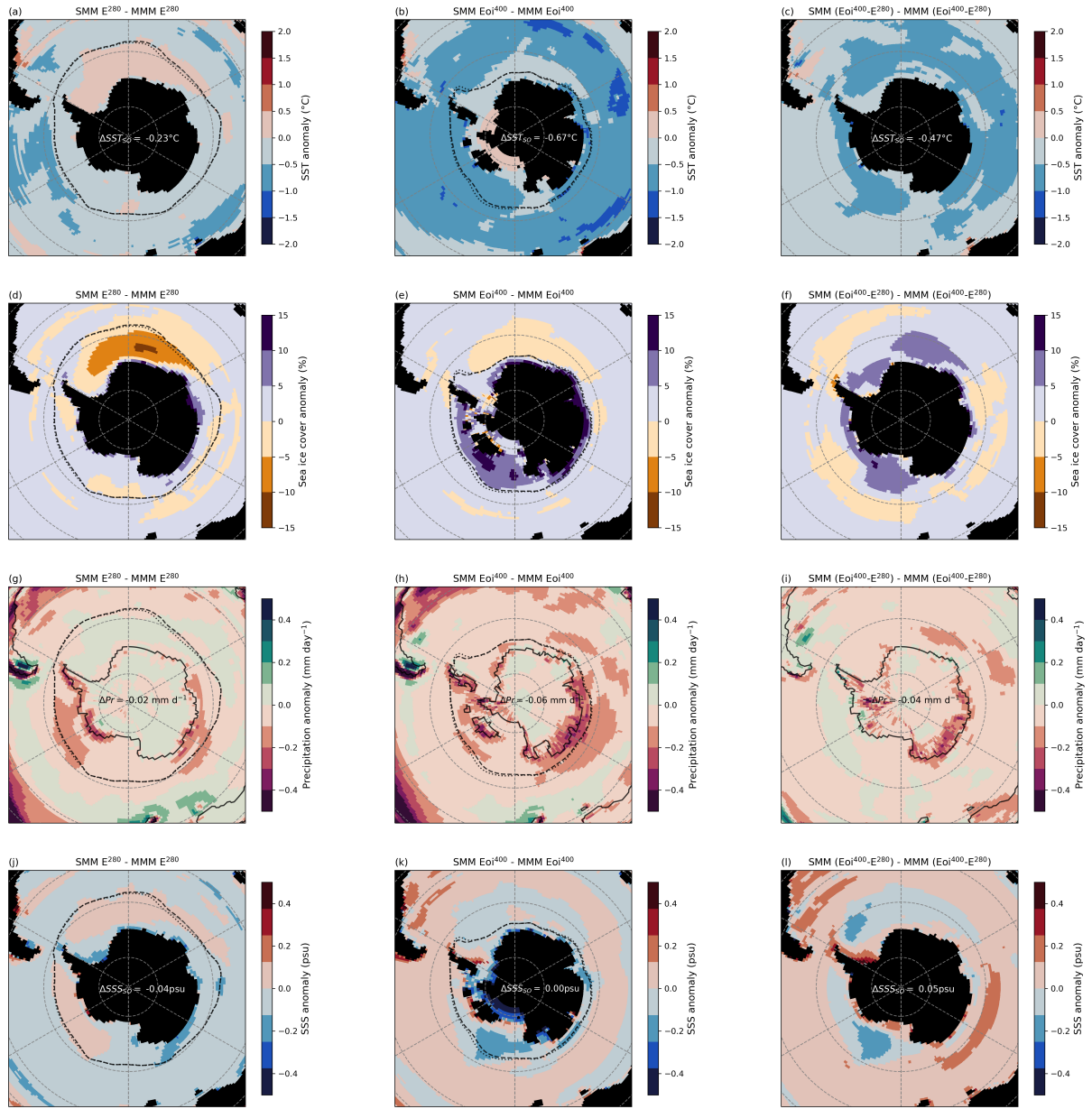
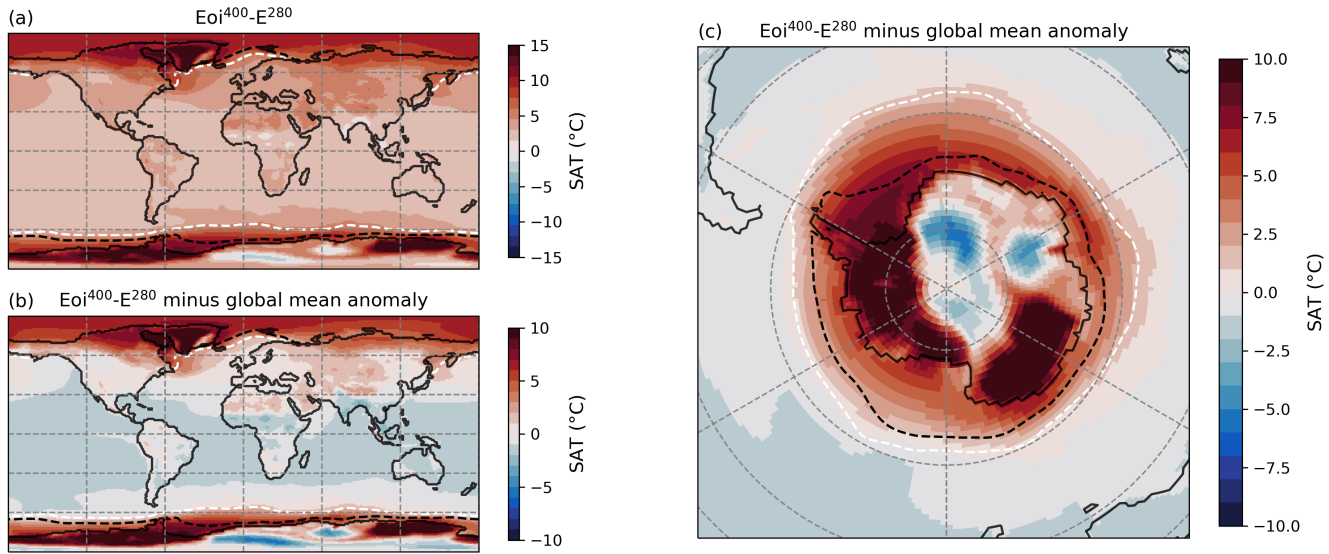


## Supplementary Tables and Figures



**Figure S1.** (a)-(c) SMM-MMM sea surface temperature (SST) anomalies for  $E^{280}$ ,  $Eoi^{400}$  and  $Eoi^{400}-E^{280}$ , respectively. Dotted and dashed lines show the SMM and MMM sea-ice edge (15% sea-ice cover). The Southern-Ocean-average SST anomaly is printed. (d)-(f) SMM-MMM sea-ice cover anomalies for  $E^{280}$ ,  $Eoi^{400}$  and  $Eoi^{400}-E^{280}$ , respectively. (g)-(i) Same as (a)-(c) for precipitation. The percentage change printed in (g), (h) and (i) is with respect to the MMM  $E^{280}$ , MMM  $Eoi^{400}$  and MMM  $Eoi^{400}-E^{280}$  precipitation, respectively. (j)-(l) Same as (a)-(c) for sea surface salinity (SSS).



**Figure S2.** (a) MMM Eoi<sup>400</sup>–E<sup>280</sup> surface air temperature (SAT) anomaly. (b) MMM Eoi<sup>400</sup>–E<sup>280</sup> SAT anomaly minus the MMM global mean SAT anomaly. (c) Same as (b) but on an orthographic projection centered in Antarctica. White and black dashed lines show the MMM sea-ice edge (15% sea-ice cover) in E<sup>280</sup> and Eoi<sup>400</sup>, respectively.

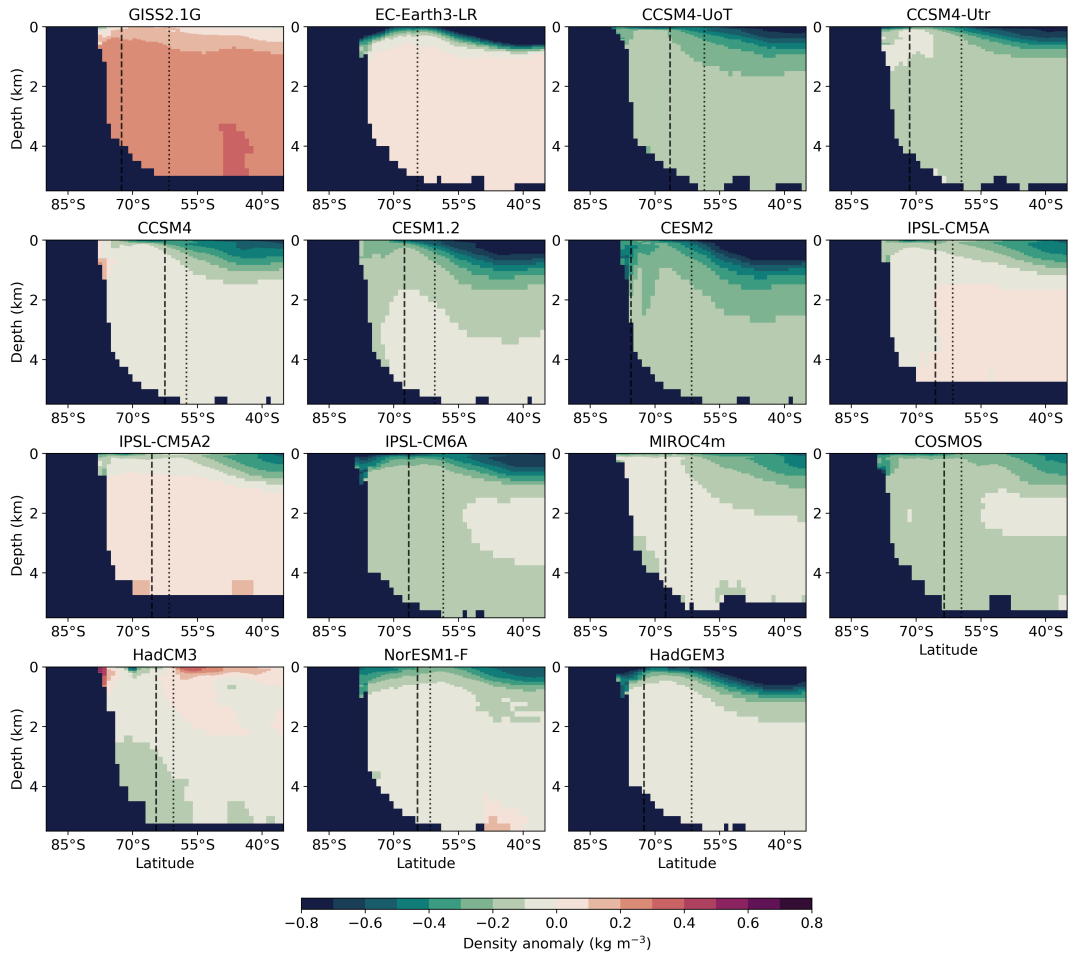


**Figure S3.** Individual model  $\text{Eoi}^{400} - \text{E}^{280}$  potential density anomalies. Vertical dotted and dashed lines indicate the MMM zonal mean sea-ice edge (15% sea-ice cover) in  $\text{E}^{280}$  and  $\text{Eoi}^{400}$ , respectively.

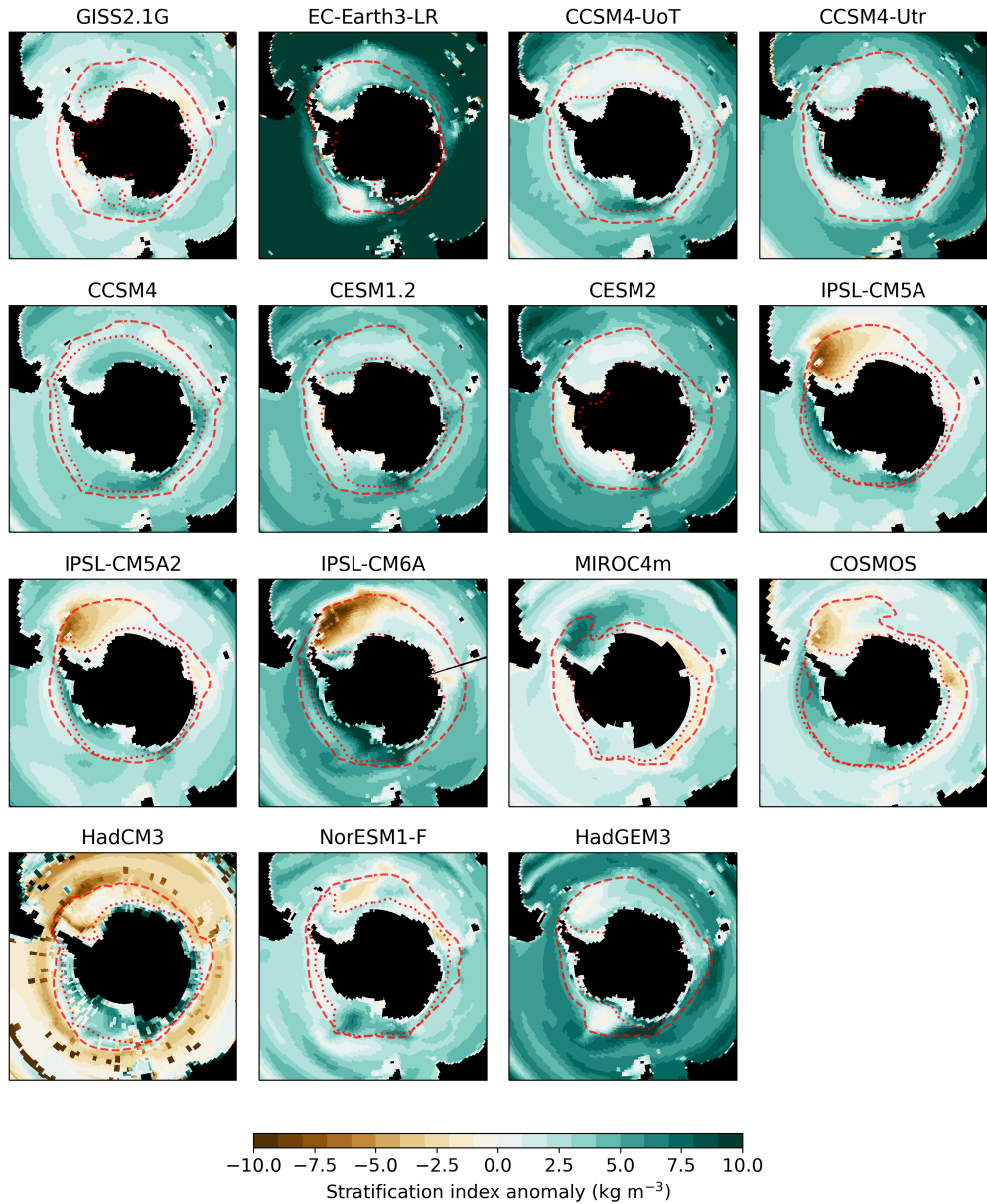


**Figure S4.** Individual model  $E^{400}$ – $E^{280}$  stratification index anomalies. Red dashed and dotted lines show the MMM sea-ice edge (15% sea-ice cover) in  $E^{280}$  and  $E^{400}$ , respectively. The stratification index is calculated for each grid cell according to Equation 1.

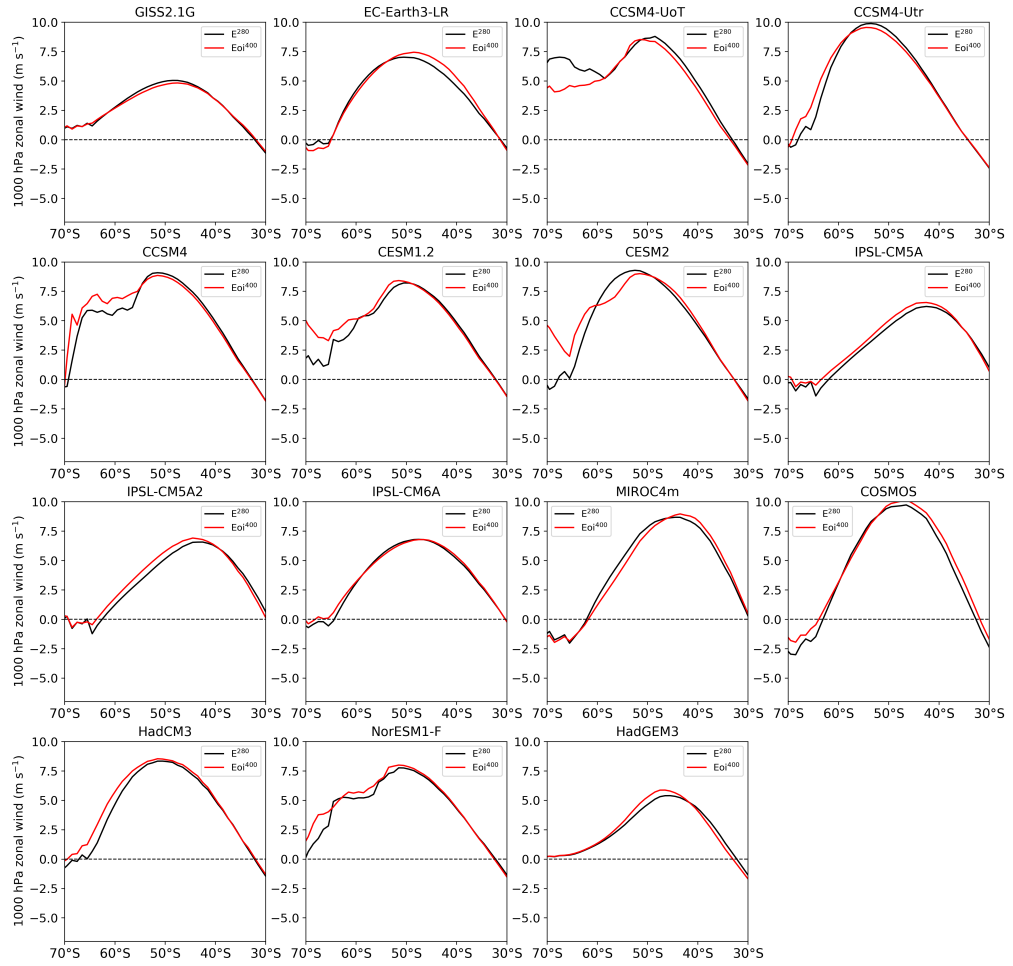


**Figure S5.** Individual model Eoi<sup>400</sup> and E<sup>280</sup> zonal-mean 1000 hPa zonal wind.

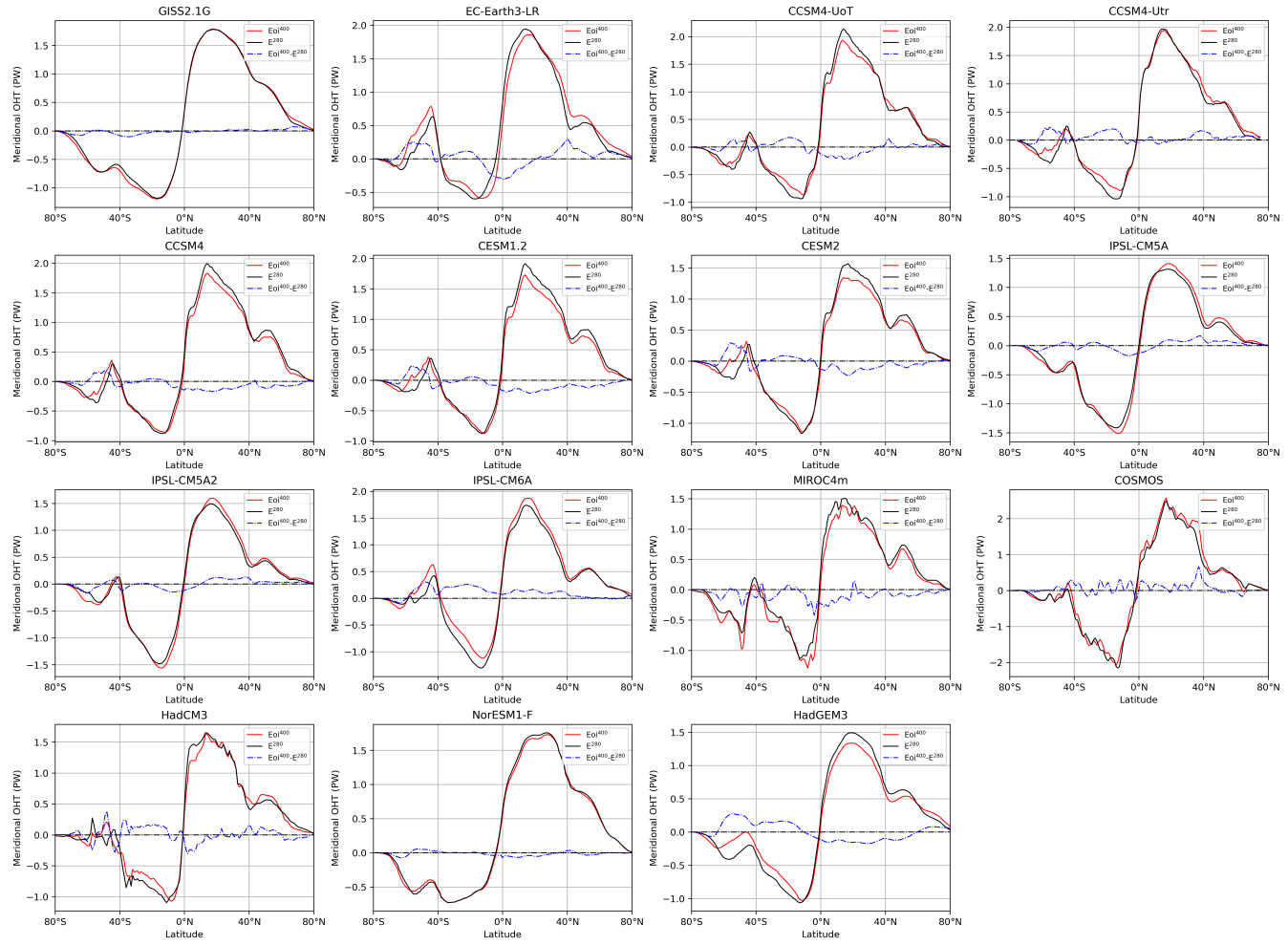


**Figure S6.** Individual model meridional ocean heat transport for  $E^{280}$ ,  $Eoi^{400}$  and  $Eoi^{400}-E^{280}$ .

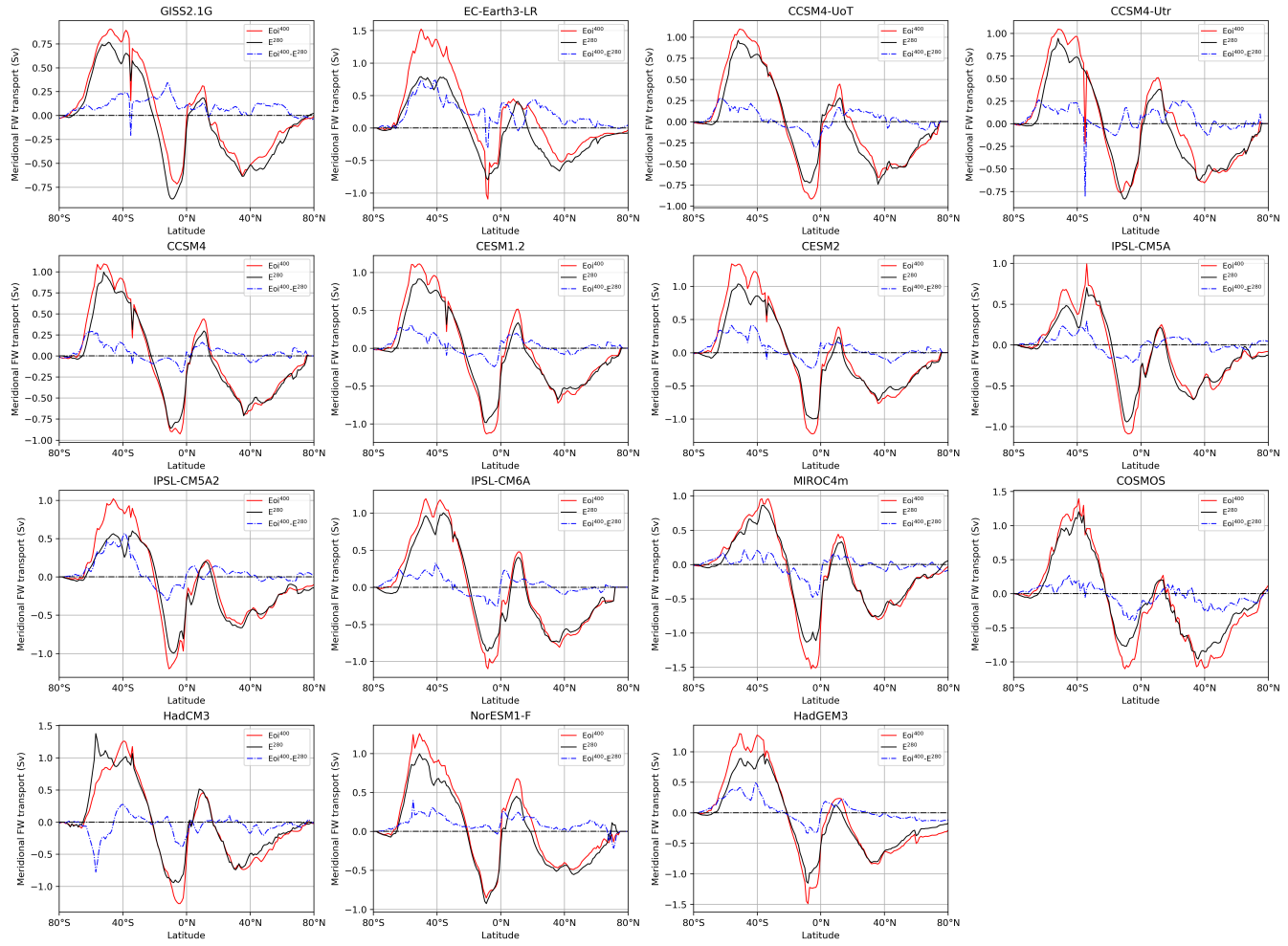


**Figure S7.** Individual model meridional freshwater transport for  $E^{280}$ ,  $Eoi^{400}$  and  $Eoi^{400}-E^{280}$ .

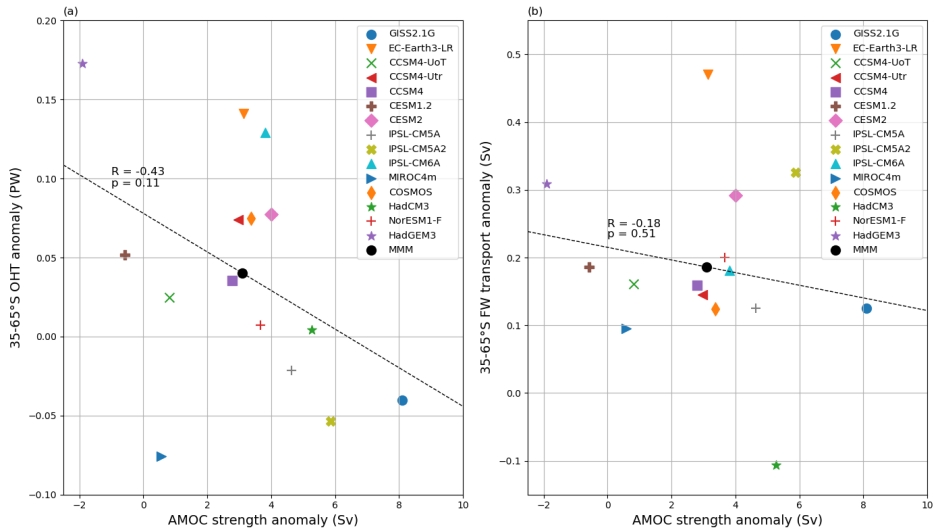


**Figure S8.** (a) Scatter plot of the individual model  $Eoi^{400}-E^{280}$  AMOC cell strength anomaly against the 35–65°S-average global ocean heat transport (OHT) anomaly. (b) Scatter plot of the individual model  $Eoi^{400}-E^{280}$  AMOC cell strength anomaly against the 35–65°S-average global freshwater transport (FWT) anomaly. Dashed lines show a linear least-squares fit to the individual model data, with indicated correlation R- and p-values.

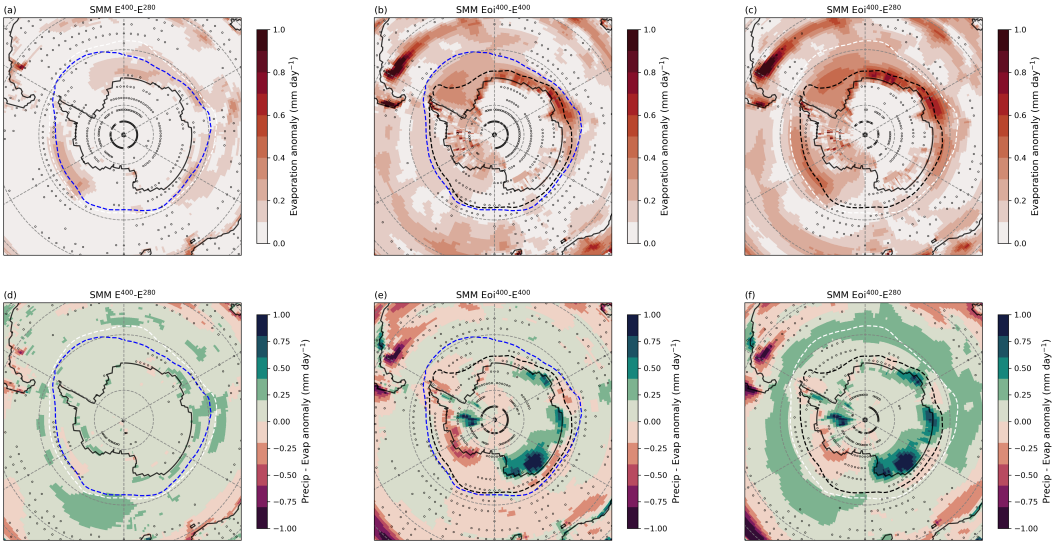


**Figure S9.** (a) SMM  $E^{400}-E^{280}$  precipitation minus evaporation (PmE) anomaly. (b),(c) Same as (a) for  $Eoi^{400}-E^{400}$  and  $Eoi^{400}-E^{280}$ . White, blue and black dashed lines show the SMM sea-ice edge (15% sea-ice cover) in  $E^{280}$ ,  $E^{400}$  and  $Eoi^{400}$ , respectively. Stippling indicates that less than 5 out of 7 ( $<70\%$ ) of the models included in the SMM agree on the sign of change.

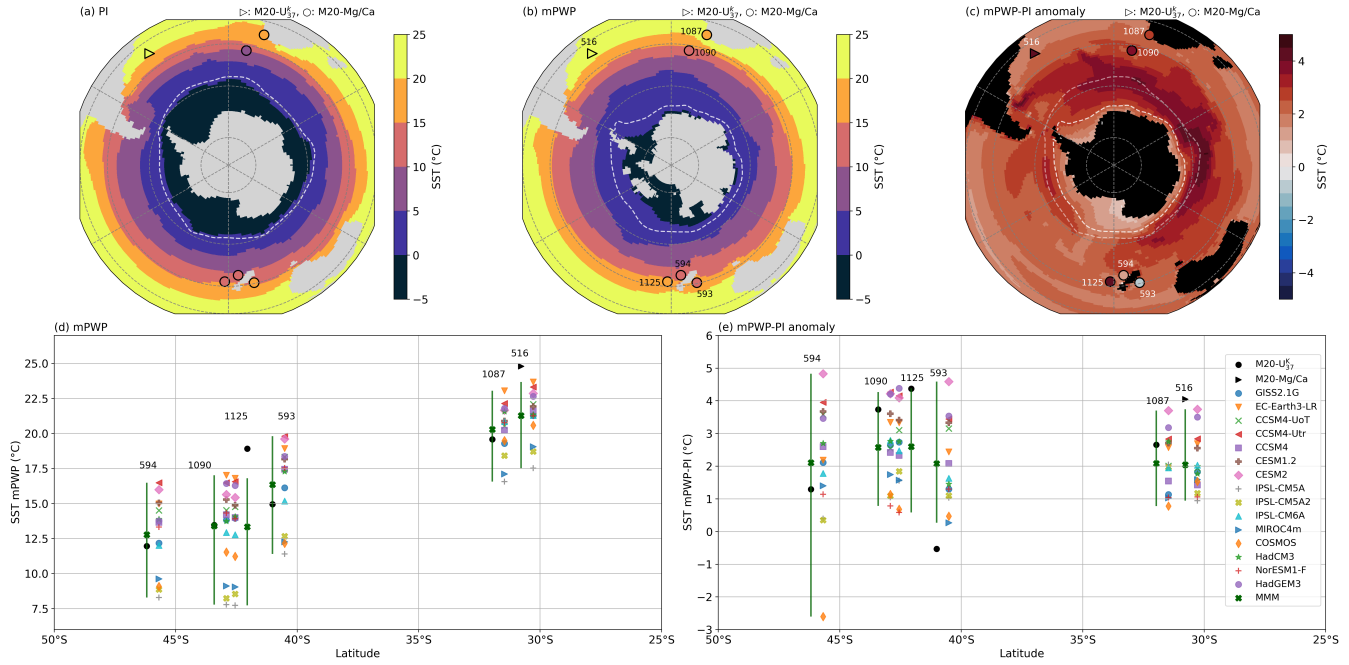


**Figure S10.** (a) Southern Ocean MMM E<sup>280</sup> SST and pre-industrial ERSSTv5 SSTs (Huang et al., 2017) at proxy locations. (b) Southern Ocean MMM Eoi<sup>400</sup> SST and KM5c mPWP SSTs reconstructed by McClymont et al. (2020) (M20) at proxy locations. M20-U<sub>37</sub><sup>k</sup> and M20-Mg/Ca refer to the McClymont et al. (2020) SST reconstructions using U<sub>37</sub><sup>k</sup> and Mg/Ca proxies, respectively. (c) Southern Ocean MMM Eoi<sup>400</sup>–E<sup>280</sup> SST anomalies and KM5c mPWP SSTs (McClymont et al., 2020) minus pre-industrial ERSSTv5 SSTs (Huang et al., 2017) at proxy locations. (d) Individual model mPWP (Eoi<sup>400</sup>) SSTs and reconstructed mPWP SSTs (black) at proxy locations in or near the Southern Ocean. A vertical dark green line shows the model spread and the MMM is indicated by a dark green cross. (e) Individual model SST anomalies (Eoi<sup>400</sup>–E<sup>280</sup>) and reconstructed mPWP-PI SST anomalies (black) at proxy locations in or near the Southern Ocean. A vertical dark green line shows the model spread and the MMM is indicated by a dark green cross. Pre-industrial SSTs are computed with the pre-industrial ERSST5 1870–1900 data (Huang et al., 2017).

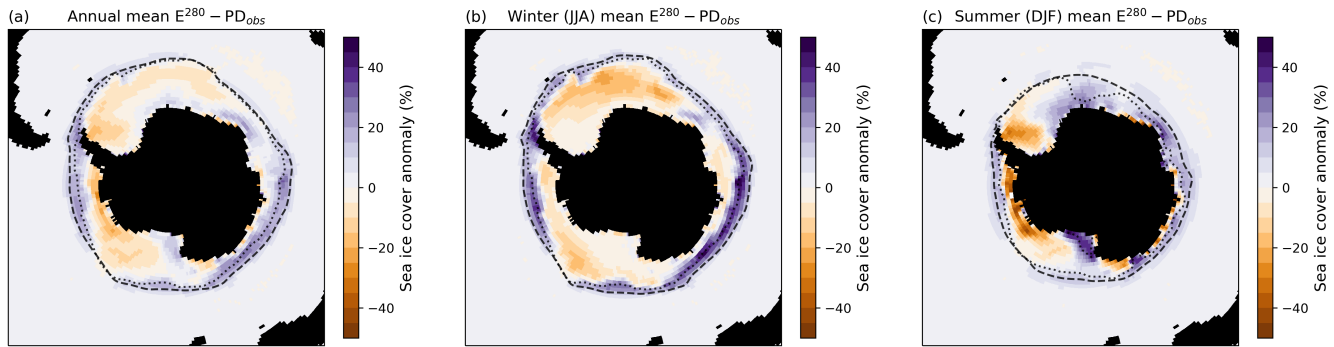


**Figure S11.** (a) Annual-mean MMM  $E^{280}$  – observed present-day ( $PD_{obs}$ , 1979–1999) sea-ice cover anomaly. (b) Winter-mean (JJA) MMM  $E^{280}$  – observed present-day ( $PD_{obs}$ , 1979–1999) sea-ice cover anomaly. (b) Summer-mean (DJF) MMM  $E^{280}$  – observed PD (1979–1999) sea-ice cover anomaly. Black dashed lines show the MMM  $E^{280}$  sea-ice edge (15% sea-ice cover) and black dotted lines show the  $PD_{obs}$  sea-ice edge.

**Table S1.** Individual model, MMM and SMM stratification index averaged over the high-latitude Southern Ocean (60–90°S).

Model	Average stratification index 60–90°S (kg m <sup>-3</sup> )				
	E <sup>280</sup>	E <sup>400</sup>	Eoi <sup>400</sup>	Eoi <sup>400</sup> – E <sup>280</sup>	E <sup>400</sup> – E <sup>280</sup>
GISS-E2.1G	4.7		5.4	0.7	
EC-Earth3-LR	5.6		10.2	4.6	
CCSM4-UoT	4.7	5.9	6.2	1.5	1.2
CCSM4-Utr	5.1		6.8	1.7	
CCSM4	5.1		7.2	2.1	
CESM1.2	7.0		8.9	1.9	
CESM2	7.9	8.9	9.4	1.5	1.0
IPSL-CM5A	3.3		4.9	1.6	
IPSL-CM5A2	3.8	4.1	5.1	1.3	0.3
IPSL-CM6A	5.9		9.0	3.1	
MIROC4m	3.7	3.7	4.5	0.8	0.0
COSMOS	3.5	4.4	5.2	1.7	0.9
HadCM3	6.7	7.5	7.1	0.4	0.8
NorESM1-F	5.1	5.9	6.8	1.7	0.8
HadGEM3	4.7		8.5	3.8	
MMM	5.1		7.0	1.9	
SMM	5.1	5.8	6.3	1.2	0.7